A Mechanism for Edge Flows and Intrinsic Toroidal Angular Momentum in Tokamaks

A. Y. Aydemir

Institute for Fusion Studies, The University of Texas at Austin, Austin, TX 78712, USA
e-mail contact: aydemir@mail.utexas.edu

Abstract. We propose a new mechanism for edge flows in tokamaks that will also serve as an intrinsic momentum source in systems without an up-down symmetry. An essential feature of toroidal plasmas is that charge-dependent ∇B and curvature drifts would lead to a vertical polarization of the discharge if it were not for the Pfirsch-Schlüter currents that neutralize the resulting charge-separation. However, in the presence of collisions, there is a residual vertical electric field that drives an $\boldsymbol{E} \times \boldsymbol{B}$ flow in the direction of increasing major radius, regardless of the orientation of the fields and currents. This flow is excluded from the hot core and is localized to the more collisional edge plasma. It has many features in common with the edge flows observed in tokamaks like C-Mod. In an up-down symmetric geometry it carries no net toroidal angular momentum; however, its viscous interaction with asymmetric boundaries leads to a net momentum input to the plasma. Both this momentum input, and the residual vertical electric field, the source of these flows, may play a role in the ∇B direction-dependence of the power threshold for the L-H transition.

1. Introduction

The tokamak edge, loosely defined in this work to be the region extending from the foot of the pedestal inside the separatrix to the inner scrape-off layer (SOL), exhibits flows documented nearly on all tokamaks[1–3]. While there are undoubtably a number of different sources for these flows, here we present a fundamental mechanism that does not seem to have drawn much attention to date.

An unavoidable feature of toroidal confinement is that charge-dependent ∇B and curvature drifts, in the absence of neutralizing flows, would set up a vertical electric field, and the resulting $\boldsymbol{E} \times \boldsymbol{B}$ drift would lead to an immediate loss of confinement. Of course with finite rotational transform, this vertical polarization and the associated electric field tend to be short-circuited by parallel currents. In a fluid model, the ∇B-dependent drifts do not appear explicitly but are subsumed by the diamagnetic current, $\boldsymbol{J}_\perp = \boldsymbol{B} \times \nabla p/B^2$, while the Pfirsch-Schlüter currents, J_{PS}, ensure charge continuity by playing the role of a neutralizing charge flow, $\nabla \cdot (\boldsymbol{J}_\perp + J_{PS}\boldsymbol{B}/B) = 0$.

With collisions, this idealized picture is modified somewhat. Although the charge continuity condition above is still satisfied in steady-state, both the diamagnetic and parallel components of the current are modified, leaving behind a residual electric field that still drives an outward (in the direction of increasing major radius, $\widehat{\boldsymbol{R}}$) $\boldsymbol{E} \times \boldsymbol{B}$-flow. However, since the hot core is essentially collisionless in modern tokamaks, this flow is confined to the more collisional edge plasma. In fact, as we will see below, higher collisionality and the presence of a pressure pedestal both play a role in this localization.

The residual electric field that results from finite collisionality points upward for a "normal" configuration of the toroidal field and current (they are both clockwise as seen from above) and reverses direction with the toroidal field, as seen in Fig. 1. In the usual toroidal coordinate system (r, θ, ζ), where θ is measured from the outboard mid-plane, and ignoring any other contributions for the moment, components of the electric field are $E_r = E_v \sin\theta, E_\theta = E_v \cos\theta$, which leads to the following poloidal flow

$$u_r = E_v B_\zeta \cos\theta / B^2, \tag{1}$$

$$u_\theta = -E_v B_\zeta \sin\theta / B^2. \tag{2}$$

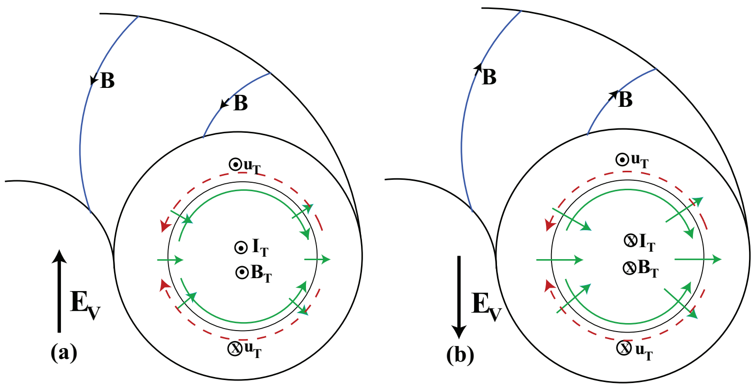

FIG. 1: A schematic description of the flows discussed here. The solid arrows represent the flows driven by the residual electric field due to polarization charges. The dashed arrows outside the separatrix (the inner solid circle) are the return flows in the SOL. (a) With the toroidal field and current in the "normal" configuration. (b) With the magnetic fields and currents reversed. Note that the electric field reverses with the $\nabla B-$drifts, but the toroidal and poloidal flows, both inside and outside, do not change direction.

For the up-down symmetric system shown in Fig. 1, the flow pattern is an exact dipole with two counter-rotating vortices localized to the edge. As it is obvious from the physics behind them, these poloidal flows are always in the direction shown. The electric field E_v reverses with the toroidal field B_ζ but the poloidal flows retain their sign. We emphatically disagree with Simakov *et al.*[4] on this point, who inexplicably insist that poloidal flows should reverse with the toroidal field. Reversal of the toroidal current has no effect on (u_r, u_θ) either. The toroidal component of the flow (labelled as u_T in Fig. 1) is given by

$$u_\zeta \simeq E_r B_\theta / B^2 = E_v B_\theta \sin\theta / B^2. \quad (3)$$

Note that u_ζ is anti-symmetric with respect to the mid-plane in the up-down symmetric geometry of Fig. 1; thus, there is no net toroidal angular momentum contribution. Unlike the poloidal flows, however, the toroidal flow changes sign either with the toroidal field (which reverses E_v), or the toroidal current (which reverses B_θ), but not when both are reversed simultaneously, as in Fig. 1. A more complete discussion of the symmetries of these flows can be found in Refs. [5, 6].

The direction of the flows outside the separatrix are determined by a global mass conservation requirement. Without the return flows, whose poloidal projection is indicated by dashed lines in Fig. 1, one would get an accumulation of material at the outside midplane. Thus, these are essentially parallel flows driven by a pressure gradient. With $\boldsymbol{u} \simeq u_\parallel \boldsymbol{B}/B$, in the upper half-plane $u_\theta > 0$ requires a positive $u_\parallel$, which also leads to $u_\zeta > 0$. Note that although the poloidal component of the flow is anti-symmetric with respect to the separatrix, the toroidal component is symmetric, having the same sign on both sides. At the bottom, the parallel flow reverses, $u_\parallel < 0$, leading to $u_\theta < 0, u_\zeta < 0$.

In this Introduction, we gave a physics overview of the flows and their general properties. In the next section, we present a more quantitative picture and discuss numerical calculations in various magnetic topologies while making comparisons with experiments, where appropriate.

2. A More Quantitative Model of the Flows

A still simplified but a somewhat more quantitative picture of these flows can be obtained by starting with the Ohm's law

$$-\nabla\phi + \nabla(V_l\zeta) = -\boldsymbol{u} \times \boldsymbol{B} + \eta\boldsymbol{J}, \tag{4}$$

where V_l is the loop voltage and ζ is the usual toroidal angle. Assuming axisymmetry, we can write $\boldsymbol{B} = \nabla\psi \times \nabla\zeta + F\nabla\zeta$, where $\psi \equiv R^2\boldsymbol{A}\cdot\nabla\zeta$, $F \equiv R^2\boldsymbol{B}\cdot\nabla\zeta$. Working in a flux coordinate system (ψ, θ, ζ) and assuming that the flows are sub-sonic, we can use the Grad-Shafranov equation $J_\zeta = -\Delta^\star\psi = FF' + R^2p'$ to replace J_ζ in the $\zeta-$component of the Ohm's law, $u^\psi \equiv \boldsymbol{u}\cdot\nabla\psi = -\eta J_\zeta + V_l$, to obtain

$$u_{rad} \equiv -u^\psi + < u^\psi >= \eta p'(R^2 - < R^2 >), \tag{5}$$

where the brackets <> denote flux surface averages and u_{rad} represents the net flow across a flux surface. (Because of the sign convention used for ψ, $\nabla\psi$ points radially inward, and p' is positive here.) Thus, there is a net radial inflow at the high-field side of the tokamak, and a net outflow on the low-field side, in agreement with Eq. 1 above.

The amplitude of the net radial flow is proportional to resistivity (Eq. 5) and at first glance might be expected to be trivially small. Note, however, the model describes physics around the separatrix (near the bottom of the pedestal), not in the hot core. Secondly, the relevant quantity is the poloidal velocity, which scales as $u_p \sim (a/\delta)u_{rad}$, where a, δ are the minor radius and flow layer width, respectively, with $a/\delta \gg 1$. It is clear from Eq. 5 that the flows are localized to the edge pedestal region where both the collisionality and pressure gradient are higher. This equation also makes the geometric origins of the flows obvious; they would not exist in a straight geometry.

3. Numerical Calculations

The flows discussed above were first observed in our attempts to find quasi-equilibrium states in the presence of various transport processes, such as viscous and resistive dissipation. There were earlier discussions of these states, but not with realistic tokamak profiles and geometries[7, 8]. The calculations use our toroidal magnetohydrodynamic (MHD) code CTD. The exact model and some of the relevant details of our calculations can be found in Refs. [5, 6] and the references therein. For the calculations reported here, a slightly generalized Ohm's law that allows for a bootstrap current contribution at the pedestal region is used. The model is ad hoc and places a narrow Gaussian layer of bootstrap current at the edge. Typically the amplitude is 20-30% of the current density on axis. Along with the temperature gradient, it helps localize the flows around the separatrix and leads to better agreement with some experimental observations. Its exact role will be discussed in an upcoming publication.

Quasi-steady state flows found with the CTD code for lower-single-null (LSN) and upper-single-null (USN) field geometries are shown in Fig. 2. Although the perfect dipole pattern of Fig. 1 is retained for a symmetric double-null configuration (not shown here), the flows are modified in an asymmetric field geometry. However, their dipole character still survives, as seen in Fig. 2(a). Note that, of the two counter-rotating vortices mentioned in the Introduction, the one away from the X-point expands in size at the expense of the other. Part of this larger vortex located in the SOL is seen to connect the low-field side of the torus to the high-field side, and eventually down (or up) to the X-point. In this simple treatment of the divertor region, that flow enters back into the plasma at the X-point, forming the inner half of the vortex that connects the X-point to the outer mid-plane. In Fig. 2(b), toroidal projection of the flows are shown along a vertical line connecting the top to the bottom of the torus approximately through its center. Although the toroidal velocity is anti-symmetric for an up-down symmetric configuration like a double-null geometry (see Fig. 1 and Eq. 3), that anti-symmetry is broken by an asymmetric field topology, as seen in the figures. Again, the portion of the flow near the X-point gets damped through its viscous interaction with the open field lines. Thus, some of the momentum is transferred to the vessel through the field lines, leaving behind a net momentum input to the plasma. Toroidal momentum transferred to the plasma is positive for LSN and negative for USN topologies, as seen in Fig. 2(b).

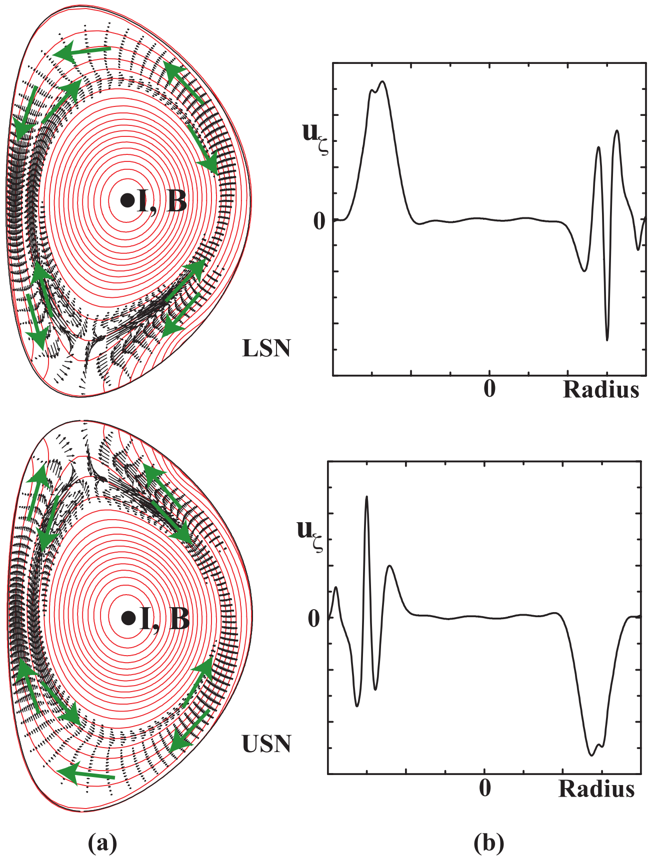

FIG. 2: Quasi-steady-state flows generated by the CTD code for upper and lower single-null magnetic geometries. Magnetic fields and current are in the "normal" direction. (a) Poloidal projections of the flows, both inside and outside the separatrix. Note that the flows retain their dipole nature (See Fig. 1), but in these asymmetric geometries, the half of the dipole flow away from the X-point expands at the expense of the other half. In both geometries there are strong flows in the SOL from the low-field to the high-field side and eventually to the X-point. (b) Toroidal projection of the flows along a vertical line passing approximately through the center and connecting the top to the bottom of the device. Here also, the portion near the X-point of the anti-symmetrix flow gets modified and damped through viscous dissipation, resulting in a net momentum input to the plasma.

In Fig. 3, reproduced from a recent article by LaBombard, *et al.*[9], the inferred SOL flows from various measurements on C-Mod are shown. For all field/current directions and magnetic topologies, our results are in qualitative agreement with these experimental observations. For the cases with the field/current in the "normal" direction, this agreement is readily apparent when the SOL flows in Figs. 2 and 3 are compared. For the two cases in Fig. 3 where the field and currents are reversed, again our results, although not shown here, are in agreement, since the transformation $\boldsymbol{B} \rightarrow -\boldsymbol{B}, \boldsymbol{u} \rightarrow +\boldsymbol{u}$ is a symmetry of our computational model[5, 6]. In other words, with the magnetic topology fixed in USN or LSN configuration, reversing all currents and fields do not alter the flows in our calculations, in apparent agreement with Fig. 3.

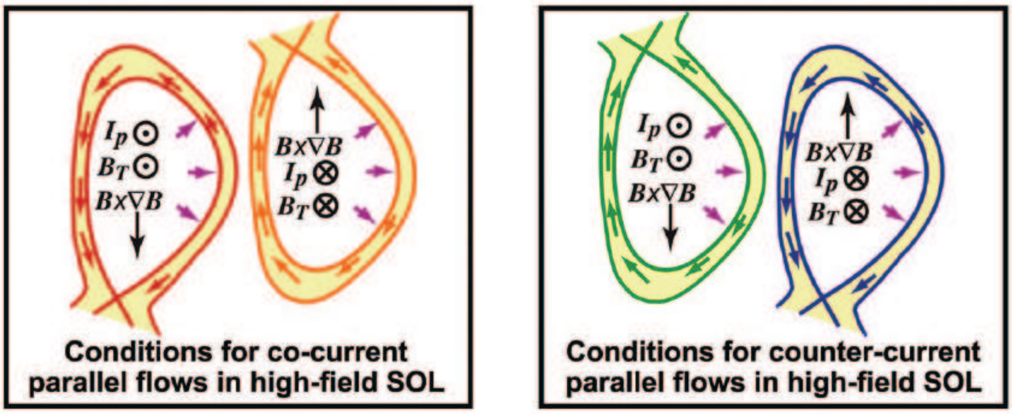

Reproduced from LaBombard *et al.*, Phys. Plasmas 15, 056106 (2008)

FIG. 3: This figure, reproduced from LaBombard et al., *Phys. Plasmas,* **15** *056106 (2008), shows the inferred SOL flows in C-Mod for various configurations. Note that for all combinations of field/current directions and magnetic topologies, our results from CTD summarized in Fig. 2 are in agreement with these experimental observations.*

4. Intrinsic Momentum Source and its Effects on the L-H Transition

The momentum input to the plasma from the SOL flows and its effect on the L-H transition power threshold has been discussed extensively by the C-Mod group (see, for example, Ref. [2]). Here, we will simply recall the dynamical origins of these effects in our model and examine its contribution in various field configurations using symmetry arguments.

As already discussed in previous sections, both the E_v-driven flows within the separatrix and the parallel return flows in the SOL have an anti-symmetric toroidal component in up-down symmetric geometries (again, see Eq. 3). But in a LSN topology, the lower portion of this toroidal flow is damped with respect to the upper, with the lost momentum being absorbed by the vessel. Since the intact upper portion is positive when the toroidal field is in the "normal" direction, there will be a net positive momentum input to the plasma. Another possibly important factor that determines the power threshold is the direction of the residual electric field E_v. Recall that the resulting radial electric field within the separatrix is $E_r = E_v \sin\theta$, which is negative approximately below the mid-plane (on the side with the X-point) and positive above. Assuming that this particular direction of E_v makes the L-H transition easier, and using this LSN with the fields in the "normal" direction as the base case, we can make the following predictions based on symmetry arguments[5, 6].

- Reversal of the toroidal field alone will increase the power threshold, since it reverses the toroidal flow, now resulting in a negative toroidal angular momentum input, and also reverses E_v (and thus E_r).
- Reversal of all fields, but still remaining in LSN, has no effect on the flows but reverses E_v, thus increasing the threshold.
- Keeping the currents and fields in the "normal" direction but switching to an USN topology will increase the threshold, since the momentum input reverses (upper, positive part of the toroidal flow gets damped), and E_v, although still positive, reverses direction with respect to the X-point.
- Note that these changes all lead to reversal of the ∇B-drift direction with respect to the location of the X-point, which is known to increase the power threshold by about a factor of two[10].

5. Summary

We demonstrated a dynamical mechanism for driving edge flows in toroidal devices. A residual vertical electric field that results from a balance between collisional effects and ∇B-dependent drifts at the plasma edge drives a toroidally outward flow within the separatrix, with an accompanying return flow outside, mainly due to parallel pressure gradients. The direction of the poloidal component of these flows is independent of the field direction; however, there is an anti-symmetric toroidal component that reverses with the toroidal field. In a symmetric system, there is no net toroidal angular momentum associated with these flows. Field and boundary asymmetries, however, can lead to a net momentum input by preferentially damping part of this anti-symmetric toroidal flow, thus providing an intrinsic momentum source. This effect and the expected reversal of the residual electric field E_v with the toroidal field have the right symmetry properties to account for the increased power threshold for the L-H transition when the ∇B-drift points away from the active X-point.

Acknowledgment: This research was supported by the Office of Fusion Energy Science of the U.S. Department of Energy under Grant DE-FG02-04ER54742.

[1] N. Asakura, S. Sakurai, K. Itami, O. Naito, H. Tagenaga, S. Higashijima, Y. Koide, Y. Sakamoto, H. Kubo, and G. D. Porter, J. Nucl. Mater. **313**, 820 (2003).

[2] B. LaBombard, J. E. Rice, A. E. Hubbard, J. W. Hughes, M. Greenwald, J. H. Irby, Y. Lin, B. Lipshultz, E. S. Marmar, C. S. Pitcher, et al., Nucl. Fusion **44**, 1047 (2004).

[3] R. A. Pitts, P. Andrew, X. Bonnin, A. V. Chankin, Y. Corre, G. Corrigan, D. Coster, I. Duran, T. Eich, S. K. Erents, et al., J. Nulc. Mater. **337**, 146 (2005).

[4] A. N. Simakov, P. J. Catto, B. LaBombard, and A. H. Glasser, Plasma Phys. Control. Fusion **50**, 105010 (2008).

[5] A. Y. Aydemir, Phys. Plasmas **14**, 056118 (2007).

[6] A. Y. Aydemir, Phys. Rev. Lett. **98**, 225002 (2007).

[7] L. P. Kamp and D. C. Montgomery, Phys. Plasmas **10**, 157 (2003).

[8] L. P. Kamp and D. C. Montgomery, J. Plasma Phys. **70**, 113 (2004).

[9] B. LaBombard, J. W. Hughes, N. Smick, A. Graf, K. Marr, R. McDermott, M. Reinke, M. Greenwald, B. Lipschultz, J. L. Terry, et al., Phys. Plasmas **15**, 056106 (2008).

[10] F. Ryter and the H-Mode Database Working Group, Nucl. Fusion **36**, 1217 (1996).